PARTICLE SWARM OPTIMIZATION-BASED CONTROL OF SHUNT ACTIVE- POWER FILTER WITH BOTH STATIC AND DYNAMIC LOADS

Essamudin A. EBRAHIM[1], Abou-Hashima EL-SAYED[2], H. I. ABDUL-GHAFFAR[3]
[1]Power-Electronics and Energy Conversion Dep., Electronics Research Institute, Egypt
[2,3]Electrical Engineering Department, Minia University, Egypt
[1]essamudin@yahoo.com, [2]dr_mostafa555@yahoo.com, [3]abdelghafar_ibrahim@yahoo.com

Abstract: *This paper introduces a design and simulation of a Shunt Active Power Filter (SAPF) for harmonic elimination of non-linear static and dynamic loads. These harmonics are generated due to non-linear industry loads based on power electronic elements and they cause enormous economic loss. The proposed SAPF uses a new artificial intelligent technique called Particle Swarm Optimization (PSO) for tuning the parameters of PI controller to achieve optimality for dc-link voltage of the SAPF-inverter. This controller is abbreviated and called PI-PSO controller. To test the robustness of the controller and the proposed system, two static and dynamic loads that fed from three-phase fully-controlled three-phase bridge rectifier are considered. The static load is an inductive load and the dynamic one is a dc separately excited dc-motor. The hysteresis non-linear current control method is used in this approach to compare the extracting reference and the actual currents in order to generate the pulse gate required for the Shunt Active Power Filter. Results obtained by simulations with Matlab/Simulink show that the proposed approach is very flexible and effective for eliminating harmonic currents generated by the non-linear loads with the shunt APF based PSO tuning. However, the total harmonic distortion (THD) is minimized and the supply power factor (PF) becomes approximately equal unity.*

Key words: *Active Power Filter, PI controller, Particle Swarm Optimization, Hysteresis current control and DC Motor model.*

1. Introduction

The need for effective control and efficient use of electric power has resulted in massive proliferation of power semiconductor processors / converters in almost all areas of electric power such as in utility, industry, and commercial applications. This has resulted in serious power quality problems, since most of these non-linear converters contribute to harmonic injection into the power system, poor power factor, unbalance, reactive power burden, etc. all leading to low system efficiency. The harmonic currents due to using the nonlinear industry loads spread into electric grid and interact adversely with a wide range of power system equipments, control systems, protection circuits, and other harmonic sensitive loads which leads to negative effect on them.

The passive filters were used to mitigate the harmonics and improve the power factor. These passive filters have disadvantages such as: resonance, the large size, insufficient fitness for large bands of harmonic frequencies which implies using of many filters, fixed compensation (very low flexibility for load variations which implies new filter design for each load variation) [1]. Among the various options available to improve power quality, the use of Active Power Filters is widely accepted and implemented as a more flexible and dynamic means of power conditioning [2-3] and many publications have represented in this subject [4-7]. Many control techniques such as instantaneous power theory [8-9], flux based controllers [10], and notch filters [11] have been introduced. Most of these control schemes are difficult to implement and require various transformations.

The SAPFs are presently the powerful tools and the most versatile and effective solution to face up to the challenge of reducing or eliminating the undesired current disturbances, protecting electrical equipment which could be affected by poor power quality and avoiding the propagation of generated disturbances to be followed toward the source or power supply[12-13].

In this paper, a SAPF is proposed to suppress harmonics due to both static and dynamic loads. The dc-link of the SAPF is controlled by using PI-controller. A new algorithm using particle swarm optimization (PSO) is proposed for tuning process of PI-controller gains (K_p and K_i). The robustness is tested by applying SAPF on both static and dynamic

loads. The static load is an inductive R-L load. In addition, a dc motor fed from thyristor controlled bridge rectifier is used as a dynamic load with a wide range for firing-angle changing from (0 to 180 degree). The hysteresis current control method is used to generate the gate pulses required for the SAPF by comparing between the actual currents and the reference currents. A simulation results by using Matlab/Software Package are obtained for several load conditions. The results show that the SAPF is a good tool for harmonic mitigation with all orders and the supply power factor is improved to unity.

2. Description of the System Under Study

Figure (1) shows the system under study. It consists of three basic units which are three-phase supply voltages, active power filter and non-linear load. These units are analyzed separately and integrated to develop the complete model for simulation.

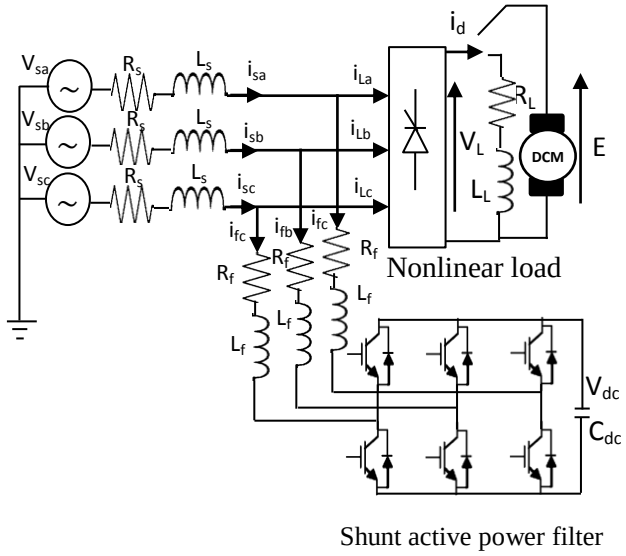

Fig. 1. Block diagram of the system with shunt APF

3. Three-Phase System Dynamic Model

3.1 Model of Three-Phase Supply Voltages

Under ideal conditions, the three-phase supply voltages are obtained by

$$\left.\begin{aligned} V_{sa} &= V_m \sin(\omega t) \\ V_{sb} &= V_m \sin(\omega t - 120) \\ V_{sc} &= V_m \sin(\omega t + 120) \end{aligned}\right\} \quad (1)$$

Where, V_m is the peak value of the supply voltage and ω is the angular frequency of the supply voltage in rad/sec.

The three-phase supply currents can be expressed as:

$$\left.\begin{aligned} i_{sa} &= i_{fa} + i_{La} \\ i_{sb} &= i_{fb} + i_{Lb} \\ i_{sc} &= i_{fc} + i_{Lc} \end{aligned}\right\} \quad (2)$$

Where, $i_{sa}, i_{sb}, i_{sc}, i_{fa}, i_{fb}, i_{fc}, i_{La}, i_{Lb}$ and i_{Lc} are the three-phase supply, SAPF, and load currents respectively.

3.2 Active Power Filter Model

APF is a power electronics device based on the use of power electronics inverters. The SAPF is connected in the point of common connection between the source of power system and the load system which present the source of the polluting currents circulating in the power system lines[14]. It is composed of a standard three-phase voltage source inverter bridge with a dc bus capacitor to provide an effective current control. The controlled currents of the SAPF are given by the following differential equations:

$$\left.\begin{aligned} pi_{fa} &= -(R_f/L_f) i_{fa} + (V_{sa} - V_{fa})/L_f \\ pi_{fb} &= -(R_f/L_f) i_{fb} + (V_{sb} - V_{fb})/L_f \\ pi_{fc} &= -(R_f/L_f) i_{fc} + (V_{sc} - V_{fc})/L_f \end{aligned}\right\} \quad (3)$$

Where, R_f and L_f are the resistance and the inductance of the APF. V_{fa}, V_{fb} and V_{fc} are three-phase APF voltages.

The DC capacitor current can be obtained in terms of three-phase APF currents as:

$$i_{dc=} i_{fa} S_a + i_{fb} S_b + i_{fc} S_c \quad (4)$$

Where, S_a, S_b and Sc are the switching functions determined by state of the APF devices.

The dc side capacitor voltage V_{dc} can be given by

$$pV_{dc} = i_{dc}/C_{dc} \quad (5)$$

The three-phase APF voltages can be determined by

$$\left.\begin{aligned} V_{fa} &= (V_{dc}/3)(2S_a - S_b - S_c) \\ V_{fb} &= (V_{dc}/3)(-S_a + 2S_b - S_c) \\ V_{fc} &= (V_{dc}/3)(-S_a - S_b + 2S_c) \end{aligned}\right\} \quad (6)$$

The shunt active power filter (SAPF) is mainly connected with the power grids to eliminate harmonics which are generated during the operation of them. The principle of SAPF is to generate compensated currents equal in magnitude and opposite in phase to those harmonic currents. This can keep the grid current in sinusoidal form and the source does not process harmonics which can enhance the system efficiency and the overall system performance.

3.3 Non-linear Load Model

3.3.1 Nonlinear Static Load Model

The nonlinear static load model comprises of three-phase controlled thyristor bridge with inductive load. the describing equations of the model are:

$$v_o = V_o(t) + \sum_{n=1}^{\infty} V_n \cos(n\omega t - \theta_n) \quad (7)$$

$$V_o(t) = \frac{3}{\pi}\int_{\theta=\alpha+\left(\frac{\pi}{3}\right)}^{\theta=\alpha+\left(\frac{2}{3\pi}\right)} \sqrt{2}\, V_L sin\theta(d\theta)$$

$$= \frac{3\sqrt{2}V_{\mathrm{m}}}{\pi} cos\alpha \quad (8)$$

$$i_o = I_o + \sum_{n=1}^{\infty} I_n \cos(n\omega t - \theta_n - \emptyset_n) \quad (9)$$

$$I_o = \frac{V_{o(t)}}{R} \quad (10)$$

$$I_n = \frac{V_n}{\sqrt{[R^2+(n\omega L)^2]}} \quad (11)$$

$$\emptyset_n = tan^{-1}\left(\frac{n\omega L}{R}\right) \quad (12)$$

Where, v_o and V_n are the instantaneous output voltage and the peak voltage of the bridge respectively. $V_o(t)$ is the DC average voltage of the bridge output. α is the firing angle and $\omega = 2\pi f$ rad/sec. V_L is the rms supply line voltage = $\sqrt{3}\, V_{ph}$. L is the load inductance (H) and R is load resistance (Ω). $\emptyset_n$ is the load angle and n is the order of harmonic.

3.3.2 Nonlinear Dynamic Load Model

The nonlinear dynamic load model consists of three-phase controlled thyristor bridge with separately excited DC motor. The model of DC motor comprises of electrical and mechanical equations as follow [15-17]:

$$u = e + R_a i + L(i)\frac{di}{dt} \quad (13)$$

$$T = T_1 + T_2 + J_{\mathrm{m}} \frac{d\omega_{\mathrm{m}}}{dt} \quad (14)$$

Where, u, e, i, R_a and L(i) are the armature voltage, back EMF, current, resistance, and inductance respectively. The inductance L(i) is a nonlinear function of current. T, T_1 and T_2 are the electromagnetic torque, the no-load torque and the load torque respectively. ω_{m} is rotational angular speed (rad/sec). J_{m} is the inertial moment of the rotator and load. The armature back EMF and the electromagnetic torque can be expressed as:

$$e = K_1 \Phi n = K_e n \quad (15)$$

$$T = K_2 \Phi i = K_T i \quad (16)$$

Where, Φ is the magnetic flux. n is the rotational speed (revolutions per minute) and $n = 60\omega/2\pi$. K_1, K_2, K_e and K_T are coefficients. T_1 is generated from the losses of the motor and can be expressed approximately as :

$$T_1 \approx T_f + T_r + T_p \quad (17)$$

Where, T_f is the friction torque, which is produced by the friction in the bearing or the friction between the brush and the commutator. T_f influences the motor startup characteristic and the startup voltage. T_r is produced by the bearing lubrication $T_r = f_r n$. T_p is produced by the aerodynamics, such as the resistance of the fan and $T_p = f_r n^2$. Therefore, the equations 17 and 18 can be rewritten as:

$$u = K_e n + R_a i + L(i)\frac{di}{dt} \quad (18)$$

$$K_T i = T_f + f_r n + f_r n^2 + T_2 + J_1 \frac{dn}{dt} \quad (19)$$

Where, $J_1 = (2\pi/60)\, J_{\mathrm{m}}$.

4. Non-linear System Model with Control Scheme

Figure (2) shows the proposed control scheme of the shunt APF. The components of this control are explained as follow:

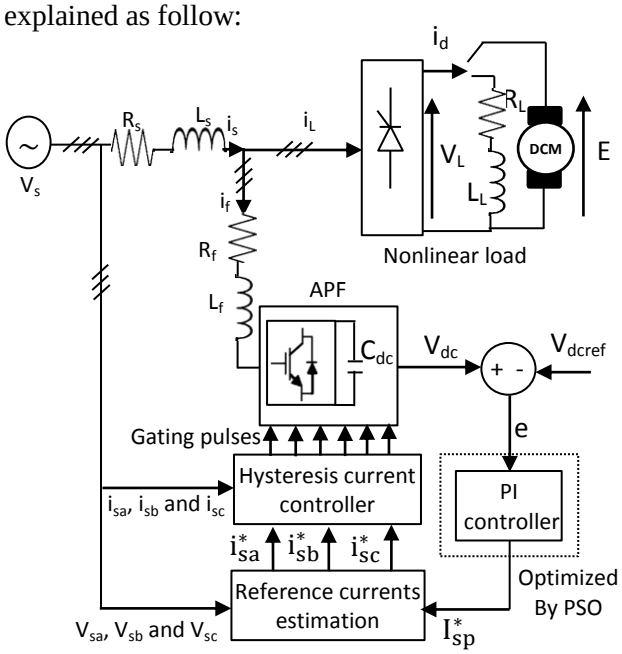

Fig. 2. The system with control scheme of SAPF

4.1 PI Controller

The PI controller is used for controlling of the SAPF to suppress the generating harmonics during the operation of the system by the injected filter currents. The DC side capacitor voltage is sensed and compared with a reference voltage. This error $e = V_{dcref} - V_{dc}$ is used as an input to PI Controller and the output is the peak value of source current (I^*_{sp}). After I^*_{sp} is obtained, it is multiplied by the unit sine vectors in phase with the respective source voltages

to obtain the reference source currents (i^*_{sa}, i^*_{sb} and i^*_{sb}). The transfer function of the PI Controller is:

$$H(s) = K_P + K_I/S \quad (20)$$

Where, K_P is the proportional constant gain and K_I is the integral constant gain. These gains are tuned by using Particle Swarm Optimization (PSO).

4.1.1 Particle Swarm Optimization (PSO)

PSO is one of the most powerful methods for solving the nonlinear optimization problems. It is basically developed through the simulation of bird flocking in two-dimension space [18-25]. Bird flocking optimizes a certain objective function. Each agent knows its best value so far (pbest) and its XY position. Moreover, each agent knows the best value so far in the group (gbest) among pbests. Each agent tries to modify its position using the following information:

1 the current position (x,y),
2 the current velocities (v_x, v_y),
3 the distance between the current position, and pbest and gbest.

The conception of modification of a searching point in Particle Swarm Optimization can be represented in Figure (3).

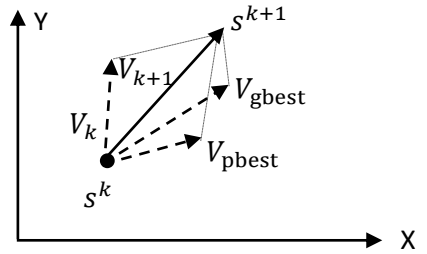

Fig. 3. Concept of modification of a searching point

Where, s^k : current searching point.
s_i^{k+1} : modified searching point.
v_k : current velocity.
v_i^{k+1} : modified velocity.
V_{gbest} : velocity based on V_{gbest}.
V_{pbest} : velocity based on V_{pbest}.

❖ **Particle Swarm Optimization Algorithm**

The steps of the PSO algorithm can be represented as follow:

Step. 1 Initialize an array of particles with random positions and their associated velocities to satisfy the inequality constraints.

Step. 2 Check for the satisfaction of the quality constraints and modify the solution if required.

Step. 3 Evaluate the fitness function of each particle.

Step. 4 Compare the current value of the fitness function with the particles previous best value (*pbest*). If the current fitness value is less, then assign the current coordinates (positions) to *pbestx.*

Step. 5 Determine the current global minimum fitness value among the current positions.

Step. 6 Compare the current global minimum with the previous global minimum (*gbest*). If the current global minimum is better than *gbest*, than assign the current global minimum to *gbest* and assign the current coordinates (positions) to *gbestx.*

Step. 7 Change the velocities according to Eq. 21.

$$v_i^{k+1} = wv_i^k + c_1\text{rand}_1\left(pbest_i - s_i^k\right) + c_2\text{rand}_2(gbest\text{-}s_i^k) \quad (21)$$

Where, $c_{1,2}$: acceleration factors.
gbest : gbest of the group.
pbest_i : pbest of agent i.
rand : random number between 0 and 1.
s_i^k :current position of agent i at iteration k.
v_i^k : velocity of agent i at iteration k.
W : weighting function.

Step. 8 Move each particle to the new position according to Eq. 22 and return to step (2).

$$s_i^{k+1} = s_i^k + v_i^{k+1} \quad (22)$$

Where, s_i^{k+1} : new current position of agent i at iteration k+1.
v_i^{k+1} : new velocity of agent i at iteration k+1.

Step. 9 Repeat Steps 2-8 until a stopping criterion is satisfied or the maximum number of iterations is reached.

The advantages of the PSO algorithm are:

1. It is easy to implement.
2. It has a limited number of parameters and the impact of parameters to the solution is small compared to other techniques.
3. The calculation in PSO algorithm is very simple.
4. It is less dependent of a set of initial points than other optimization methods.

❖ **Flowchart of Particle Swarm Optimization**

The steps of the Particle Swarm Optimization algorithm can be represented by the flowchart shown in Figure (4).

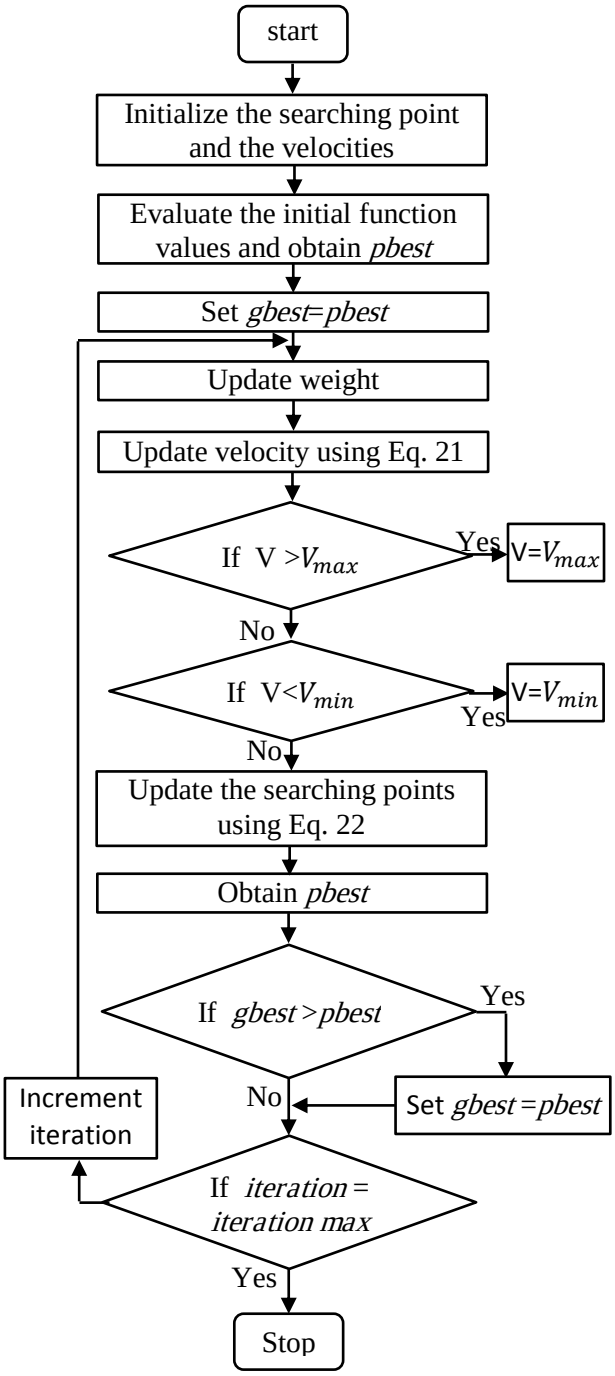

Fig. 4. Flowchart of Particle Swarm Optimization

4.2 Reference Source Currents Estimation

The rms source voltage amplitude (V_{sm}) is calculated from the three-phase source voltages (V_{sa}, V_{sb} and V_{sc}) by

$$V_{sm} = \sqrt{\frac{2}{3}(V_{sa}^2 + V_{sb}^2 + V_{sc}^2)} \quad (23)$$

The direct (or in-phase) unit current vectors are given from the three- phase source voltages and the rms source voltage amplitude (V_{sm}) as expressed in the following equations.

$$\left.\begin{aligned} u_{sa} &= V_{sa}/V_{sm} \\ u_{sb} &= V_{sb}/V_{sm} \\ u_{sc} &= V_{sc}/V_{sm} \end{aligned}\right\} \quad (24)$$

The reference three-phase source currents (i_{sa}^*, i_{sb}^* and i_{sc}^*) are estimated as:

$$\left.\begin{aligned} i_{sa}^* &= I_{sp}^* u_{sa} \\ i_{sb}^* &= I_{sp}^* u_{sb} \\ i_{sc}^* &= I_{sp}^* u_{sc} \end{aligned}\right\} \quad (25)$$

Where, I_{sp}^* is the peak value of the source current which is the output of the PI controller.

4.3 Hysteresis Non-linear Current Controller

This method provides instantaneous current corrective response, good accuracy and unconditioned stability to the system. Also, it aims to keep the controlled current inside a defined rejoin around the desired reference current [9]. In this method, the reference and actual three-phase source currents are compared with each other to obtain the gating pulses to the devices of APF. The current controller decides the switching pattern of the APF devices. The switching logic is determined as follows:

If $i_{sa} < (i_{sa}^* - HB)$ for leg "a" (S_a=1), the upper switch is OFF and the lower switch is ON.

If $i_{sa} > (i_{sa}^* + HB)$ for leg "a" (S_a=0), the upper switch is ON and the lower switch is OFF.

The switching functions S_b and S_c which are phases leg "b" and leg "c" respectively are formulated similarly by the measured currents (i_{sb} and i_{sc}), the corresponding reference currents (i_{sb}^* and i_{sc}^*) and the hysteresis bandwidth (HB). The hysteresis control principle and the gate pulse can be represented in Figure (5).

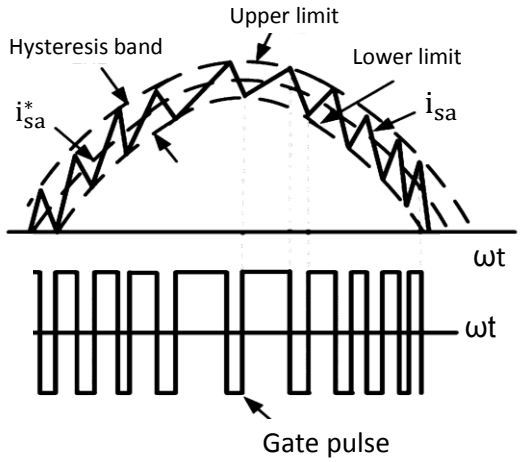

Fig. 5. Hysteresis Control Principle

5. Objective Function

In this paper, the PSO is used for obtaining the coefficients of PI controller K_P and K_i. The main object of the optimal PI controller design is eliminating the harmonic currents generated by the nonlinear load in the electric grid. The integral of squared error (ISE) is considered as the cost function to be minimized. The objective function is given as:

$$J=\int_0^{\infty}(e^2)dt \quad (26)$$

Where (J) is the cost function and (e) is the error which evaluated from the following Equation.

$$e = V_{dcref} - V_{dc} \quad (27)$$

Therefore, the design problem can be formulated as the following optimization problem.

Minimize J Subject to

$$Z^{min} \leq Z \leq Z^{max} \quad (28)$$

Where Z is a vector, which consists of the parameters of the PI controller. The proposed approach employs PSO to search for the optimal set of PI controller coefficients which leads to minimize the total harmonic distortion.

6. Simulation Results and Discussions

To test the robustness and validation of the proposed controller in harmonic mitigation, several static and dynamic loads fed from semiconductor switches with distorted supplies are supposed and used. First, an inductive static load (RL) fed from silicon fully controlled rectified thyristor bridge is simulated and tested. The load resistance and conductance used equal (R= and L=). The thyristor parameters are given in the appendix. Also, a separately excited DC motor fed from the same thyristor bridge is used as a dynamic load. The motor is loaded by two different mechanical load torques. The first one is applying a load torque that directly proportional to motor speed and the second proportional to square value of motor speed. Test motor parameters are given in appendix.

Matlab/Simulink program is used in a simulation process. All simulation results include: the supply current before and after using SAPF, the phase shift between the supply current and voltage to show the improvement in power factor, THD, SAPF currents, motor starting running and steady state currents, motor internal and load torques and DC link actual and reference voltages. This results are severely obtained for different values of firing angle.

6.1 Non-linear Static Inductive Load

6.1.1 Without Shunt Active Power Filter

The supply current of phase A and its total harmonic distortion is represented in Figure (6). The current (Id) after the controlled bridge is obtained in Figure (7).

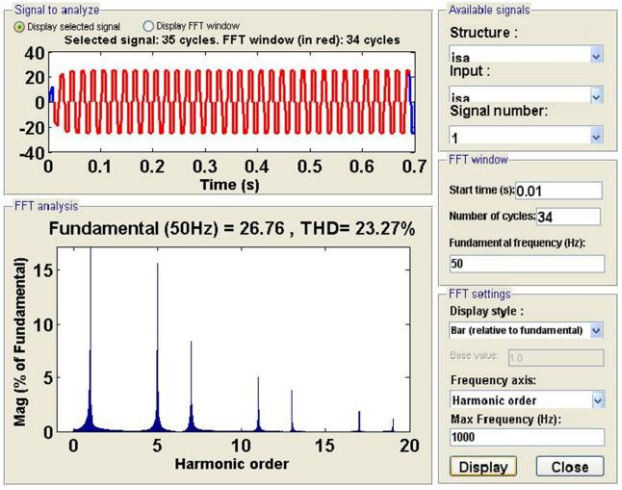

Fig. 6. Supply current (i_{sa})

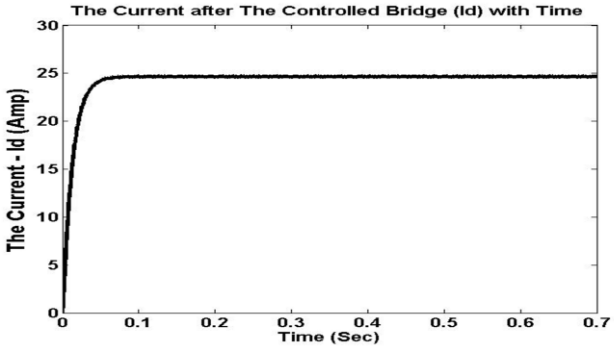

Fig. 7. Current (I_d) after the controlled bridge

The results show that the system is affected by the nonlinear load during the operation. Where, the Total Harmonic Distortion (THD) of the supply current (i_{sa}) is high and equals 23.27% at firing angle=0 degree.

6.1.2 Static Inductive Load With SAPF

The PSO is used for PI controller tuning, the optimum parameters are obtained by PSO where K_P =1.6 and K_i = 16. Figure (8) shows the supply current (i_{sa}) and its Total Harmonic Distortion.

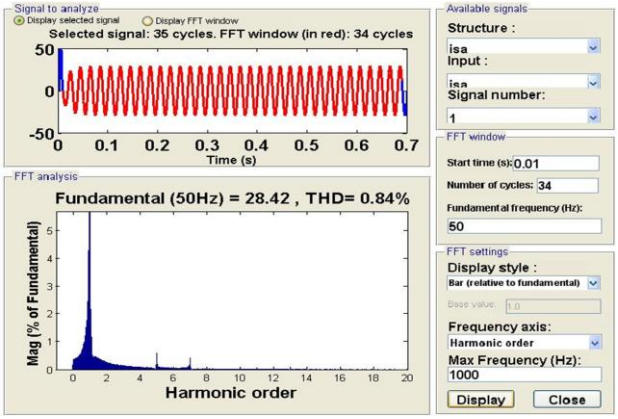

Fig. 8. Supply current (i_{sa})

The filter current (i_{fa}) is obtained in Figure (9). A comparison between the THD response of the supply and load currents is represented in Figure (10). The current I_d is shown in Figure (11). The response of actual DC-link voltage matches well its reference with zero steady state error as shown in Figure (12). Figure (13) shows both supply voltage and current waveforms. It can be noted that there is no phase shift between supply voltage and current waveforms. This mains that the SAPF improves PF to unity.

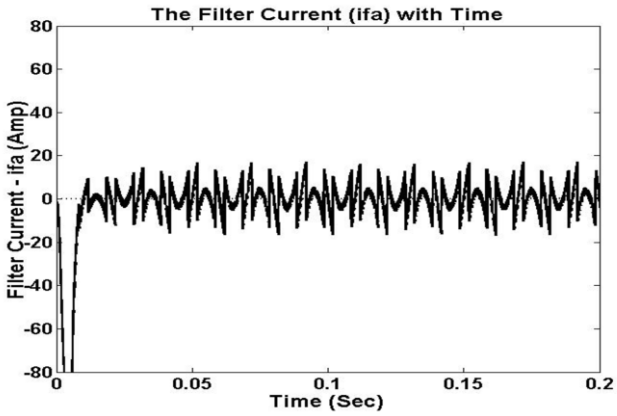

Fig. 9. Filter current (i_{fa})

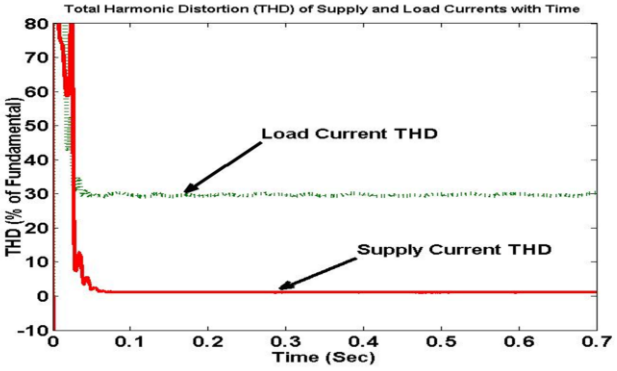

Fig. 10. Total Harmonic Distortion (THD)

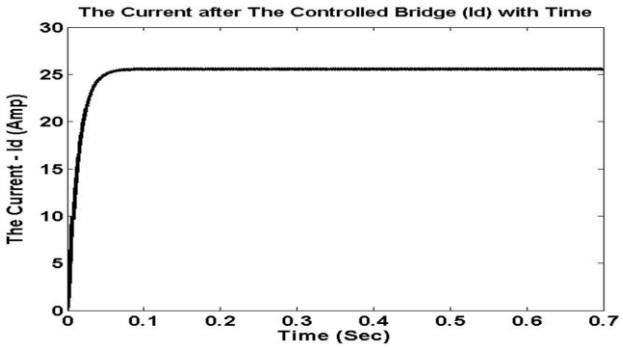

Fig. 11. Current (I_d) after the controlled bridge

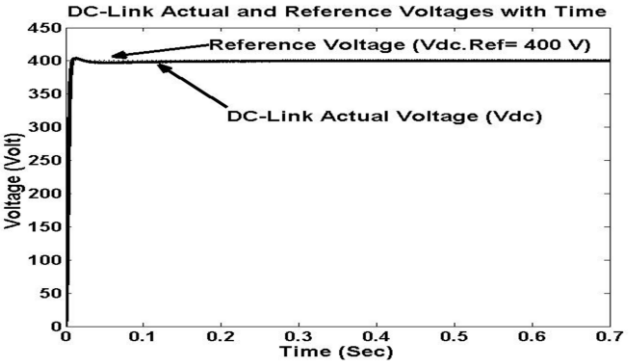

Fig. 12. DC-Link reference and actual voltages

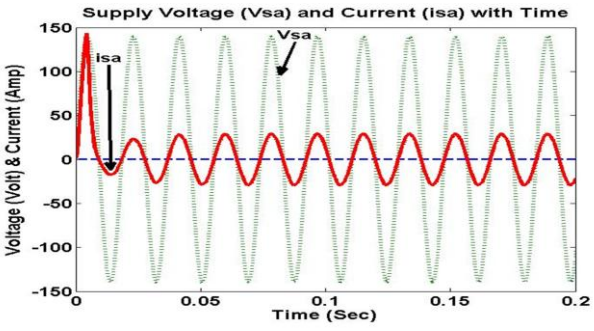

Fig. 13. Phase shift of supply voltage and current waveforms

From the results, the system behavior is improved and its performance is enhanced when it is connected to the shunt APF controlled by PI controller based PSO tuning. This intelligent controller makes better performance for the system in facing the generated harmonics during the operation. There is marked improvement in shape of the supply current and the Total Harmonic Distortion as shown in Table 1. This proves that the Shunt Active Power Filter based Particle Swarm Optimization has strong effectiveness for harmonics elimination and improvement the overall power system performance. Table (1) represents a comparison between the THD of the supply current at different values of the firing angle before and after using SAPF based PI-PSO tuning.

Tab. 1. THD% with and without using SAPF for the supply phase current

Firing Angle (∝)	0	30	60	90
THD without using SAPF	23.27%	28.32%	30.11%	37.92%
THD with using SAPF	0.84%	2.87%	8.44%	11.33%

6.2 DC Motor Dynamic Load

This section includes simulation results for DC motor fed from thyristor bridge with different load torques.

6.2.1 Load Torque (T_L) Directly Proportional to Speed (ω_n)]

In this subsection, the case under study is the three phase controlled bridge connected to the DC motor.

The load torque (T_L) is considered as a function in angular velocity (ω_m) in rad/sec where $T_L=K_1*\omega_m$ and $K_1=0.1143$.

6.2.1.1 With Proposed PI- PSO SAPF

The simulation results are obtained when using the proposed PI-PSO SAPF to study its effect when using it. Figure (14) shows the supply current and its Total Harmonic Distortion (THD) after connecting the SAPF controlled by PI controller tuned by PSO.

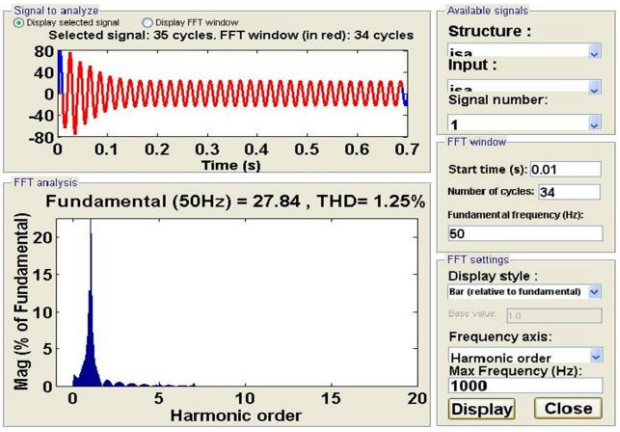

Fig. 14. Supply current (i_{sa})

The optimum parameters of the PI controller are obtained by PSO where Kp=1.6 and Ki=70. Figure (15) shows the filter current and a comparison between the THD of supply and load currents can be expressed in Figure (16). The motor armature current I_a, motor speed (ω_m), load torque (T_L) and internal electrical torque (T_e) are shown in Figures (17) to (20) respectively. Figure (21) represents the response of the actual DC link voltage that tracks its reference with zero steady state error.

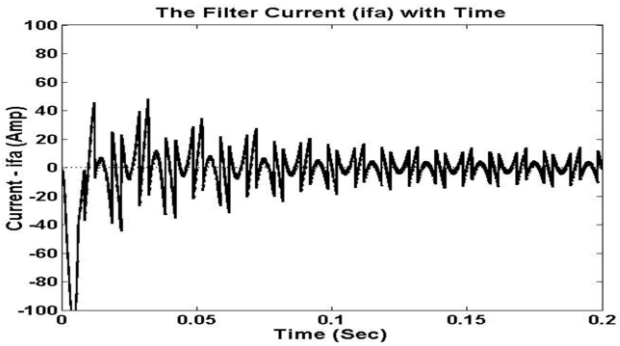

Fig. 15. Filter current (i_{fa})

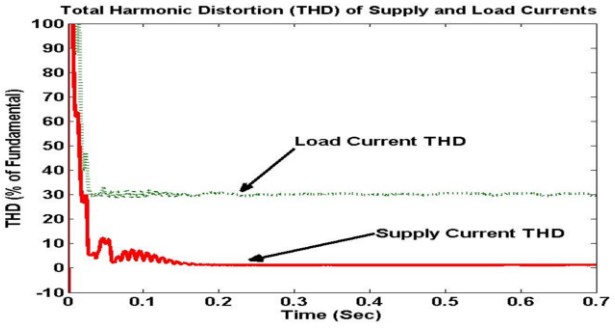

Fig. 16. Total Harmonic Distortion (THD)

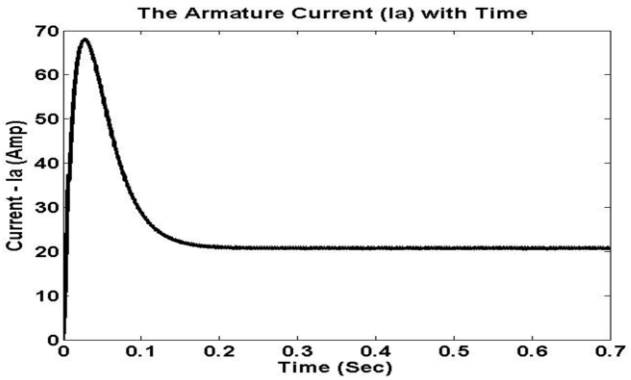

Fig. 17. Armature current (I_a)

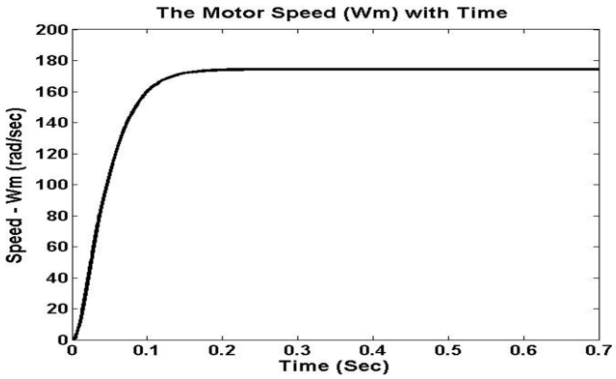

Fig. 18. Motor speed (ω_m)

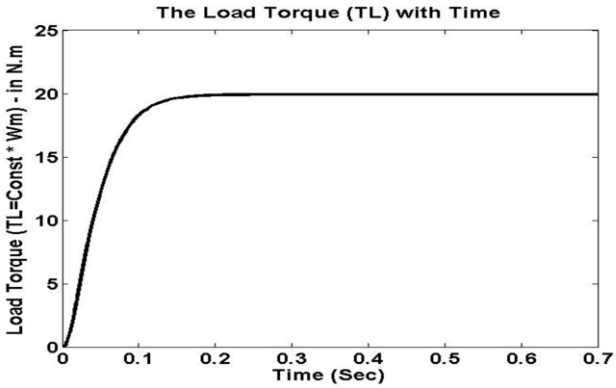

Fig. 19. Load torque (T_L)

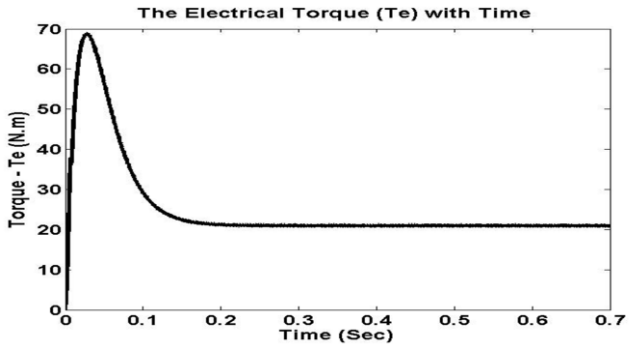

Fig. 20. Electrical torque (T_e)

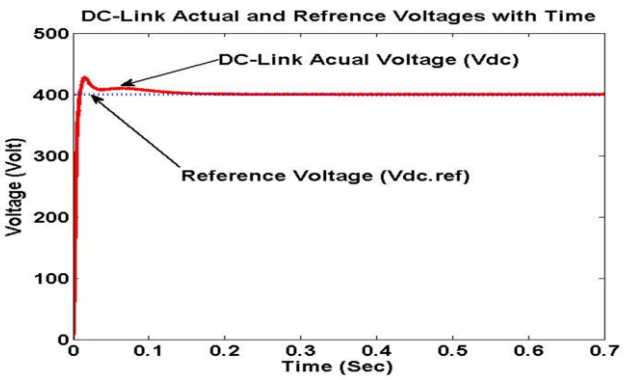

Fig. 21. DC-Link actual and reference voltages

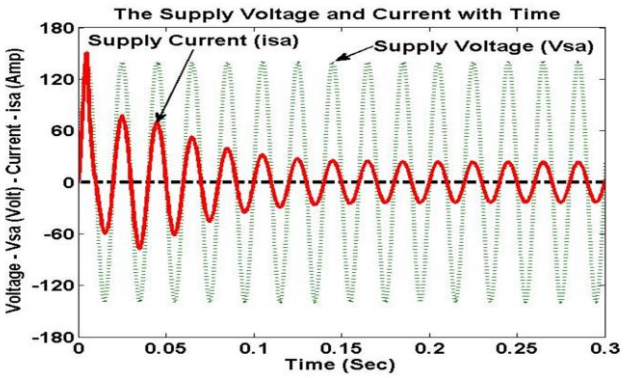

Fig. 22. Supply voltage (V_{sa}) and Current (i_{sa})

From the results, the system behavior is improved and its performance is enhanced when using the proposed SAPF with PI-PSO controller. The THD is decreased to 1.25% at firing angle (α=0). The supply current waveform is approximately pure sine wave. The power factor is reached to the unity as shown in Figure (22). There is marked improvement in the system behavior for different values of the firing angle as shown in Table (2).

Tab. 2. THD% of the supply phase current with and without using SAPF

Firing Angle (∝)	0	30	60	90
THD% without using SAPF	24.13%	29.18%	31.21%	38.34%
THD% with using SAPF	1.25%	2.47%	8.73%	11.97%

6.2.2 Load Torque (T_L) As A function in Speed Square (ω_n^2)

In this subsection, the load torque (T_L) is considered as a function in the square of angular velocity (ω_m^2) in rad/sec where $T_L=K_2*\omega_m^2$ and K2=6.87e^{-4}.

6.2.2.1 With PI –PSO SAPF

The SAPF filter is controlled by the PI controller tuned by PSO. Figure (23) shows the supply current and its Total Harmonic Distortion (THD). The filter current is represented in Figure (24).

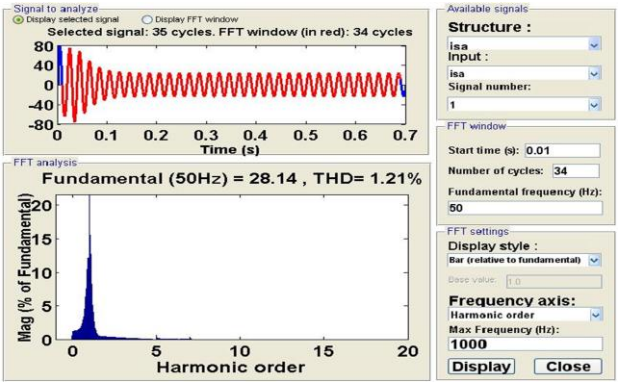

Fig. 23. Supply current (i_{sa})

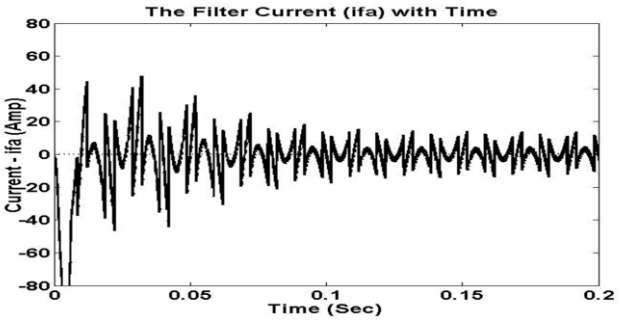

Fig. 24. Filter current (i_{fa})

The optimum parameters of the PI controller are obtained by PSO where Kp=1.6 and Ki=70. A comparison between the THD of supply and load currents can be expressed in Figure (25). The motor armature current (I_a), internal electrical torque (T_e), motor speed (ω_m) and load torque (T_L) are shown in Figures (26) to (29) respectively. Figure (30) shows a comparison between the DC-link actual and reference voltages. A comparison between supply voltage and current is expressed in Figure (31).

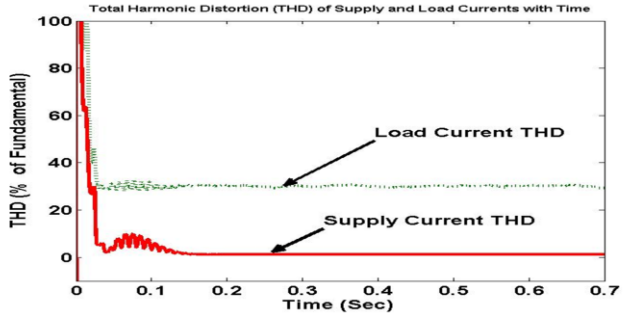

Fig. 25. Total Harmonic Distortion (THD)

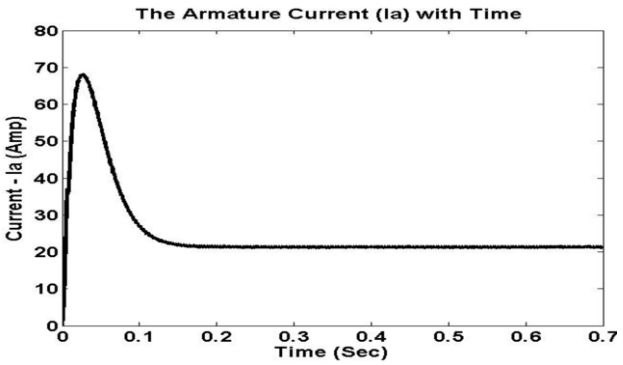

Fig. 26. Armature current (I_a)

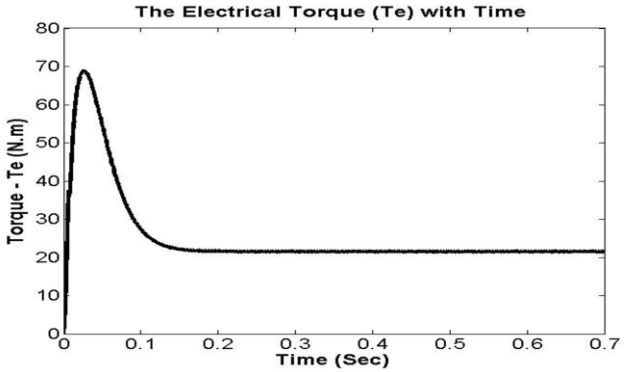

Fig. 27. Electrical torque (T_e)

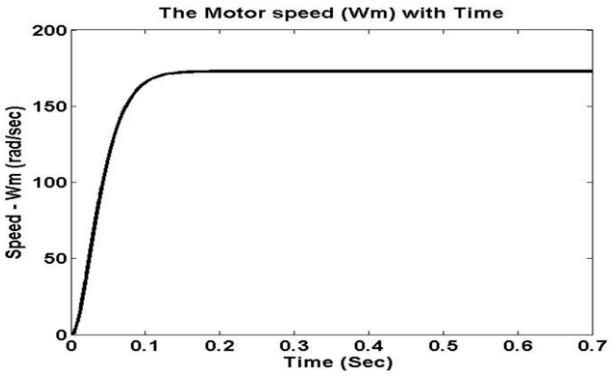

Fig. 28. Motor speed (ω_m)

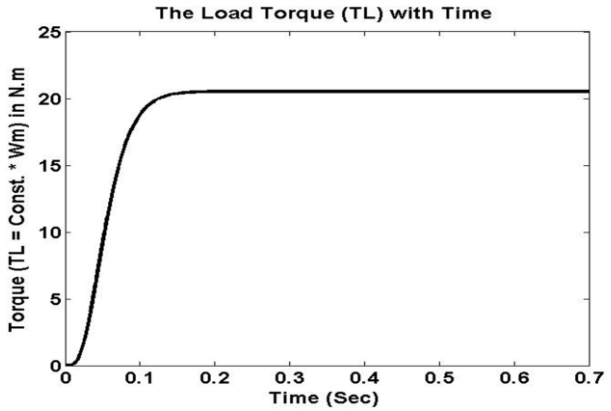

Fig. 29. Load torque (T_L)

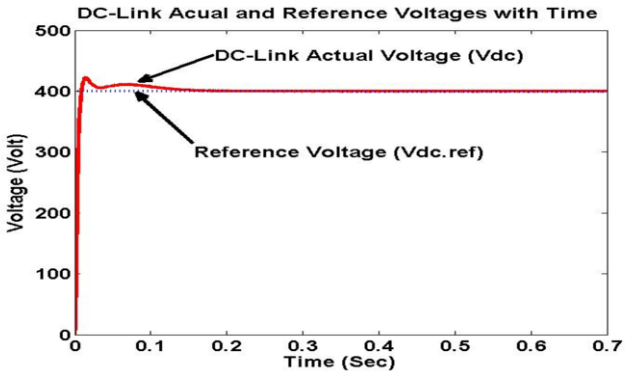

Fig. 30. DC-Link actual and reference voltages

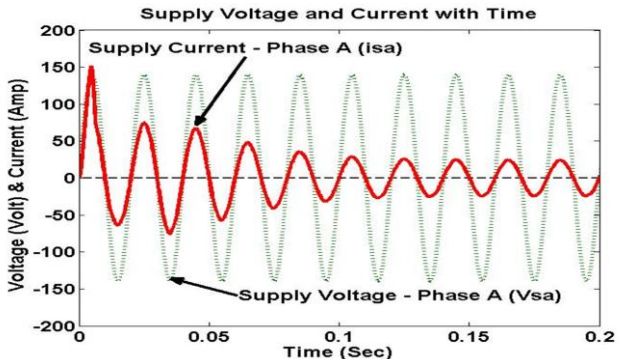

Fig. 31. Supply voltage and current

The results show that the Total Harmonic Distortion (THD) is decreased which means that enhanced in the system behavior and its performance when it is connected to the shunt APF controlled by PI controller based PSO tuning. The THD is decreased to 1.05% at firing angle (α=0). Also, waveform of the supply current is improved and approximately becomes pure sine wave. Then, the power factor is improved and approximately increased to unity as shown in Figure (31). There are different values of the THD for (α) as shown in Table (3).

Tab. 3. THD% of the supply line current with and without using SAPF

Firing Angle (∝)	0	30	60	90
THD% without using SAPF	24.1%	29.24%	31.37%	38.62%
THD% with using SAPF	1.05%	3.136%	9.11%	12.13%

7. Conclusion

In this paper, SAPF is proposed and introduced as a solution for harmonics mitigation. The dc- Link voltage of the SAPF is controlled using PI controller. An intelligent technique called PSO is suggested for fine tuning and optimization of PI parameters. This filter is abbreviated as PI-PSO SAPF.

The robustness of the controller is tested by applying two problem loads with the proposed filter. Both static inductive and dynamic loads with different load torque operations are fed from fully controlled thyristor bridge rectifier with a wide range of firing angle variation. From simulation results, THD for supply phase current is decreased from 23.27% to 0.84% for Static inductive load when using the proposed PI-PSO SAPF. In case of dynamic DC motor load, the THD is minimized from 24.13% to (1.05%:1.25%) for all motor loading conditions. This proves that using the proposed PI-PSO SAPF gives good promotion for its use in the harmonics elimination of the nonlinear electric grids.

References

1. B. Singh, K. Al-Haddad and A. Chandra.: *A new control approach to three-phase active filter for harmonics and reactive power compensation*. In: IEEE Transactions on Power Systems, Vol. 13, No. 1, February 1998, p. 133-138.
2. S. Rahmani, K. Al-Haddad & F. Fnaiech.: *A three-phase shunt active power filter for damping of harmonic propagation in power distribution networks.* In: Proc. IEEE International symposium on Industrial Electronics, Vol. 3, July 2006, p. 1760-1764.
3. B. N. Singh.: *Design and Digital Implementation of Active Filter with Power Balance Theory*. In: IEEE Proc on EPA, Vol. 2, No. 5, September 2005, p.1149-1160.
4. Z. Chen, Y. Luo and M. Chen.: *Control and performance of a cascaded shunt active power filter for aircraft electric power system*. In: IEEE Transactions on Industrial Electronics, Vol. 59, No. 9, September 2012, p. 3614-3623.
5. Q. Trinh and H. Lee.: *An advanced current control strategy for three phase shunt active power filters*. In: IEEE Transactions on Industrial Electronics, Vol. 60, No. 12, December 2013, p. 5400-5410.
6. A. F. Zobaa.: *Optimal multi-objective design of hybrid active power filters considering a distorted environment*. In: IEEE Transactions on Industrial Electronics, Vol. 61, No. 1, 2014, p. 107-114.
7. P. Acuna, L. Moran, M. Rivera, J. Dixon and J. Rodriguez.: *Improved active power filter performance for renewable power generation systems*. In: IEEE Transactions on Power Electronics, Vol. 29, No. 2, 2014, p. 687-694.
8. H. Akagi.: *New trends in active filters for improving power quality*. In: IEEE-PEDES Conference Record, January 22-24, 1996, p. 417-425.

9. H. Akagi, Y. Kanazwa and A. Nabae.: *Instantaneous reactive power compensators comprising switching devices without energy storage components*. In: IEEE Transactions on Industry Applications, Vol. IA-20, No. 3, 1984, p. 625-630.
10. S. Bhattacharya, A. Veltman, D. M. Divan and R. D. Lorenz.: *Flux based active filter controller*. In: IEEE-IAS Annual Meeting, 1995, p. 2483-2491.
11. M. Rastogi, N. Mohan and A. A. Edris.: *Hybrid active filtering of harmonic currents in power systems*. In: IEEE Transactions on Power Delivery, Vol. 10, No. 4, October 1995, p. 1994-2000.
12. S. G. Jeong and J.-Y. Choi: *Line current characteristics of three-phase uncontrolled rectifiers under line voltage unbalance condition*. In: IEEE Trans. on Power elect., Vol. 17, 2002, p. 935-945.
13. M. Bauta and M. Grötzbach: *Noncharacteristic line harmonics of AC/DC converters with high DC current ripple.* In: IEEE Transactions Power Delivery, Vol. 15, 2000, p. 1060-1066.
14. H. Akagi and A. Nabae: *Control strategy of active power filters using multiple voltage source PWM converters.* In: IEEE Transactions Industry Applications, Vol. IA-22 1986, p. 460-465.
15. X. Liu, H. Zhang, J. Liu, J. Yang.: *Fault detection and diagnosis of permanent-magnet DC motor based on parameter estimation and network*. In: IEEE Transactions on Industrial Electronics, Vol. 47, No. 5, 2000, p. 1021-1025.
16. A. J. Viji, T. A. Victoire.: *Power quality improvement by UPQC with fuzzy logic controller. In:* Journal of Electrical Engineering, Vol. 15, Edition 1, January 2015, p. 55-63.
17. K. Habib, A. Alam,S. Khan, R. Amin, S. M. Ali.: *average current control mode boost converter for the tuning of total harmonic distortion & power factor correction using PSIM. In:* Journal of Electrical Engineering, Vol. 15, Edition 1, January 2015, p. 287-292.
18. J. Kennedy and R. Eberhart.: *Particle swarm optimization*. In: Proc. IEEE Int. Conf. Neural Networks, 1995, Australia, Vol. 4, p. 1942–1948.
19. J. Kennedy.: The Particle swarm : Social adaptation of knowledge. In: Proc. IEEE Int. Conf. on Evol. Comput., 1997, Indianapolis, Vol. 4, p. 303–308.
20. Y. Shi and R. Eberhart.: *A modified particle swarm optimizer*. In: Proc. IEEE International Conference Evol. Comput., May 1998, Anchorage, AK, p. 69–73.
21. Y. Shi and R. C. Eberhart.: *Empirical study of particle swarm optimization*. In: Proceeding IEEE International Conference Evolution Computations, July 1999, Washington, DC, p. 1945–1950.
22. M. A. Abido.: *Optimal design of power system stabilizers using particle swarm optimization*. In: IEEE Transactions on Energy Conversion, Vol.17, Issue 3, September 2002, p. 406-413.
23. N. K. Sharma, D. S. Babu and S. C. Choube.: *Application of particle swarm optimization technique for reactive power optimization*. In: IEEE Int. Conference on Advances in Engineering, Science and Management, March 30-31, 2012, p. 88-93.
24. L. G. Rodriguez, S. L. Perez, J. F. Mora.: *Particle swarm optimization applied in power system measurement-based load modeling*. In: IEEE Conf. on Evolutionary Computation, June 20-23, 2013, Cancun, p. 2368-2375.
25. H. I. Abdul-Ghaffar, E. A. Ebrahim, M. Azzam.: *Design of PID controller for power system stabilization using particle swarm-bacterial foraging optimization*. In: WSEAS Transactions on Power Systems, Vol. 8, Issue 1, January 2013, p. 12-23.

Appendix

- The system parameters:

	Nonlinear system parameters	Value
1	Three phase source voltage, V_s	100 V
2	Frequency, f	50 Hz
3	Source resistance, R_s	0.1Ω,
4	Source inductance, L_s	0.15mh
5	Load resistance, R_l	9Ω
6	Load inductance, L_l	110mH
7	Filter resistance, R_f	0.1Ω,
8	Filter inductance, L_f	0.335mH
9	DC Capacitance, C_{dc}	2000 µF
10	DC Reference Voltage, V_{dc}	400 V

- The Particle Swarm Optimization parameters:

1	PSO parameter (C1)	1.2
2	PSO parameter (C2)	0.12

- The motor parameters:

Motor model: 5HP-240V-1750PM-Field 300V

	Motor parameters	Value
1	Armature resistance, R_a	2.581 Ω
2	Armature inductance, L_a	0.028 H
3	Field resistance, R_f	281.3 Ω,
4	Field inductance, L_f	156 H
5	Field-armature mutual inductance, L_{af}	0.9483 H
6	Total inertia, J	0.02215 $kg.m^2$
7	Viscous friction coefficient, B_m	0.002953 .m.s
8	Coulomb friction torque, T_f	0.5161 N.m